NASA/TM-20240002690

Joining, Disassembly, and Reconfiguration of Thermoplastic Composites for Space Applications

Joseph Pinakidis and Sandi Miller
Glenn Research Center, Cleveland, Ohio

May 2024

NASA STI Program Report Series

Since its founding, NASA has been dedicated to the advancement of aeronautics and space science. The NASA scientific and technical information (STI) program plays a key part in helping NASA maintain this important role.

The NASA STI program operates under the auspices of the Agency Chief Information Officer. It collects, organizes, provides for archiving, and disseminates NASA's STI. The NASA STI program provides access to the NTRS Registered and its public interface, the NASA Technical Reports Server, thus providing one of the largest collections of aeronautical and space science STI in the world. Results are published in both non-NASA channels and by NASA in the NASA STI Report Series, which includes the following report types:

- TECHNICAL PUBLICATION.
  Reports of completed research or a major significant phase of research that present the results of NASA Programs and include extensive data or theoretical analysis. Includes compilations of significant scientific and technical data and information deemed to be of continuing reference value. NASA counterpart of peer-reviewed formal professional papers but has less stringent limitations on manuscript length and extent of graphic presentations.

- TECHNICAL MEMORANDUM.
  Scientific and technical findings that are preliminary or of specialized interest, e.g., quick release reports, working papers, and bibliographies that contain minimal annotation. Does not contain extensive analysis.

- CONTRACTOR REPORT.
  Scientific and technical findings by NASA-sponsored contractors and grantees.

- CONTRACTOR REPORT.
  Scientific and technical findings by NASA-sponsored contractors and grantees.

- CONFERENCE PUBLICATION.
  Collected papers from scientific and technical conferences, symposia, seminars, or other meetings sponsored or co-sponsored by NASA.

- SPECIAL PUBLICATION.
  Scientific, technical, or historical information from NASA programs, projects, and missions, often concerned with subjects having substantial public interest.

- TECHNICAL TRANSLATION.
  English-language translations of foreign scientific and technical material pertinent to NASA's mission.

Specialized services also include organizing and publishing research results, distributing specialized research announcements and feeds, providing information desk and personal search support, and enabling data exchange services.

For more information about the NASA STI program, see the following:

- Access the NASA STI program home page at http://www.sti.nasa.gov

NASA/TM-20240002690

Joining, Disassembly, and Reconfiguration of Thermoplastic Composites for Space Applications

Joseph Pinakidis and Sandi Miller
Glenn Research Center, Cleveland, Ohio

National Aeronautics and
Space Administration

Glenn Research Center
Cleveland, Ohio 44135

May 2024

Acknowledgments

The authors would like to acknowledge Dr. Witold Fuchs for his contribution to this work and input related to polymer science.

Level of Review: This material has been technically reviewed by technical management.

This report is available in electronic form at https://www.sti.nasa.gov/ and https://ntrs.nasa.gov/

NASA STI Program/Mail Stop 050
NASA Langley Research Center
Hampton, VA 23681-2199

Joining, Disassembly, and Reconfiguration of Thermoplastic Composites for Space Applications

Joseph Pinakidis and Sandi Miller
National Aeronautics and Space Administration
Glenn Research Center
Cleveland, Ohio 44135

Summary

Thermoplastic composites are increasingly being investigated for aerospace applications because of their relatively short processing time, good chemical and radiation resistance, and potential for reforming and reuse via melting. The manufacturing, reforming, and reuse of thermoplastic composites can be leveraged to advance joining, disassembly, and reassembly of structures for space exploration activities. Potential applications include, but are not limited to, habitats and on-orbit assembly and/or reassembly of large-scale truss structures.

This work focuses on demonstrating the feasibility of joining, disassembly, and reassembly of a thermoplastic bond using heat and pressure. Polyether ether ketone (PEEK) composite adherends were joined using polyphenylene sulfide (PPS) and low-melt polyaryl ether ketone (LM-PAEK) thermoplastic films at the bonding interface. Once consolidated, each unique material system was evaluated for shear strength and interlaminar separation force at both room (23 °C) and elevated (121 °C) temperature. Shear strength was calculated through single-lap shear tests, and interlaminar separation force was found utilizing a modified three-point bend test. Both the PPS and LM-PAEK films were found to have a maximum shear strength between 3 and 8 MPa and consistently failed adhesively at the bondline. The shear strength could be increased by integrating a ply of LM-PAEK prepreg into the composite adherend to facilitate entanglement and increase bonding, but at the cost of a more random and catastrophic failure mode.

Reassembly of disassembled specimens was successfully demonstrated using additional thermoplastic interlayers. Thus, the reassembly of thermoplastic composite joints was found to be feasible. However, additional work is required to reduce film flowout, potential film degradation, and optimization of consolidation parameters in a space environment.

Acronyms

ET	elevated temperature
FFPD	film-forming polymeric dispersion
GF	glass fiber
GFRP	glass-fiber-reinforced plastics
GnP	graphene nanoplates
LM	low melt
MWCNT	multiwall carbon nanotube
PAEK	polyaryl ether ketone
PEEK	polyether ether ketone
PP	polypropylene
PPS	polyphenylene sulfide
RT	room temperature

SLS single-lap shear
TPC thermoplastic composite
TSC thermoset composite

1.0 Introduction

Composites are attractive for aeronautics and space applications due to their high strength-to-weight ratio and geometric tailorability (Ref. 1). Historically, thermoset composites (TSCs) have dominated composite use in aerospace because of their lower raw material cost, better defined manufacturing and repair processes, and lower processing temperature and pressure compared to those of thermoplastics (Ref. 2). However, thermoplastic composites (TPCs) offer many advantages, including reduced cycle time and increased production rate, reformability and reusability, high fracture toughness and durability, and good chemical, ultraviolet, and radiation resistance (Refs. 3 and 4). The manufacturing benefits of TPCs can be leveraged for space applications such as habitats and on-orbit assembly and reassembly of large-scale truss structures. However, the feasibility of reconfiguration and its effects on mechanical performance must be better understood before it becomes a viable option.

Fusion bonding and disassembly of dissimilar materials (TPCs, TSCs, and metals) is achieved either by coprocessing a thermoplastic film to the adherend or by using a hybrid interlayer (Ref. 5). De Weert investigated the disassembly of fusion-bonded TPC joints using induction heating, finding that induction heating to 130 °C caused a 37-percent reduction in force required to separate the single-lap shear (SLS) specimens with minimal edge defects (Ref. 6). Larger reductions in force were achieved at higher temperatures but at the cost of thermal damage to the specimen. The co-consolidated panels with a susceptor mesh interface at the joint were easier to disassemble but had a lower strength at room temperature (RT). Notably, ultrasonically welded coupons were the most difficult to disassemble because the welded joint interface acted as a thermally insulative layer. This is an important finding that may limit the use of this emerging technology for this application.

The process of ultrasonic welding to join TPCs has promising potential but has not been thoroughly investigated for space application. Work by Frederick, Li, and Palardy explored the disassembly of ultrasonically welded TPCs using an electrically conductive multiwall carbon nanotube (MWCNT) film. A process of resistance heating was used to disjoin the specimen. It was found that at an elevated temperature (ET) of 130 °C and 20 wt% MWCNT/polypropylene (PP), the lap shear strength of the joint decreased by approximately 90 percent (Ref. 7). This finding is of interest because a reduction in strength with targeted heating could be beneficial to an application such as in-orbit disassembly and reassembly. Palardy et al. investigated (1) the processing parameters necessary for ultrasonic consolidation of TPCs using experimental and finite element modeling, (2) heat generation effects at joint interface, and (3) the effect of energy director thickness on heat dissipation to the adherend (Refs. 8 to 11). Haq et al. demonstrated the joining and disassembly of glass-fiber-reinforced plastics (GFRPs) using a thermoplastic Nylon 6 sheet with and without graphene nanoplates (GnP) at the bondline. It was shown that using microwave radiation was sufficient to induce the heat to 240 °C and separate the lap shear joint. In addition, an introduction of 3 wt% GnP increased the lap shear strength by approximately 155 percent (Ref. 12). The addition of GnP was not investigated in this report but could be an area of future work to improve thermal conductivity of the film. Koutras studied the effect of ET on resistance-welded glass fiber/polyphenylene sulfide (GF/PPS) joints with a stainless steel heating element and found a 22-percent decrease in lap shear strength at 120 °C, with a local cohesive failure mode of the PPS film at its fracture line (Ref. 13). Although the PPS film is similar to the one used in this report, Koutras's study differs in

that both the adherend and adhesive were made of PPS and above their glass transition temperature T_g at time of failure and the joint incorporated a heating element, whereas this report does not.

The purpose of this report is to evaluate the feasibility of the joining, disjoining, and reassembly of carbon fiber/polyether ether ketone (PEEK) TPCs using PPS and low-melt polyaryl ether ketone (LM-PAEK) interlayer films. These materials were chosen because they are high-performance, space-application-relevant thermoplastics. The interlayer material was varied, and performance was characterized using a modified three-point bend test and SLS tests. Interlayer thickness and failure mode were recorded as well. Finally, rejoining of SLS joints was attempted and mechanical properties were characterized to better understand the transferability of this process to future space applications such as on-orbit reassembly.

2.0 Methods

2.1 Materials and Specimen Preparation

2.1.1 Carbon-Fiber-Reinforced Panels

Prepreg plies of AS4 carbon fiber with the semicrystalline thermoplastic PEEK Cetex® TC1200 unidirectional tape was obtained from Toray Advanced Composites. Likewise, prepreg plies of T700 carbon fiber with semicrystalline thermoplastic LM-PAEK Cetex® TC1225 was obtained from Toray Advanced Composites. Fortron® (Fortron Industries LLC) PPS 0214 powder from Celanese and LM-PAEK powder from Victrex (AE™ 250 FFPD25) were used to fabricate films to be used at the bondline.

AS4/PEEK quasi-isotropic adherends were compression molded using a $[45/0/–45/90]_{2s}$ ply configuration for the lap shear specimen and a $[0]_8$ ply configuration for the three-point bend test. AS4/PEEK prepreg was laid up in a picture frame tool and compression molded at 393 °C and 0.34 MPa for 1 h. The cooldown rate was maintained between 10 and 20 °C/min to ensure crystallization within the matrix. The panels were then cut to size with a diamond saw cutter. A similar process was repeated for the hybrid composite panel in a $[45/0/–45/90]_{2s}$ configuration except that the bottom and top layers were substituted to be T700/LM-PAEK prepreg plies before compression molding. The hybrid panel was pressed at 382 °C, 0.34 MPa, for 1 h.

2.1.2 Thermoplastic Film Interlayer

PPS film was fabricated by pressing 10 g of PPS powder between sheets of polyimide tape coated in mold release in a hot press at 316 °C for 10 min with approximate applied pressure ranging from 0.14 to 0.77 MPa. This created a flat sheet that still had slight variations in thickness due to processing. Therefore, only sections that varied in thickness from 0.10 to 0.12 mm were used. To create thicker films, more powder was used and pressed for shorter amounts of time.

LM-PAEK film was fabricated by pressing 20 g of powder at 329 °C for 10 min with approximate applied pressure ranging from 0.10 to 0.51 MPa. The resulting film also varied in thickness so sections that were from 0.08 to 0.15 mm thick were used.

2.1.3 Lap Shear Specimen Preparation

Lap shear test coupons were assembled in a steel frame and aligned with balancing shims and spacers. The lap shear joint was formed by compression molding at 329 °C and 0.14 MPa for 30 min. This process was repeated to prepare joints for the three-point bend test. The joining process for both SLS and three-point bend panels is pictured in Figure 1.

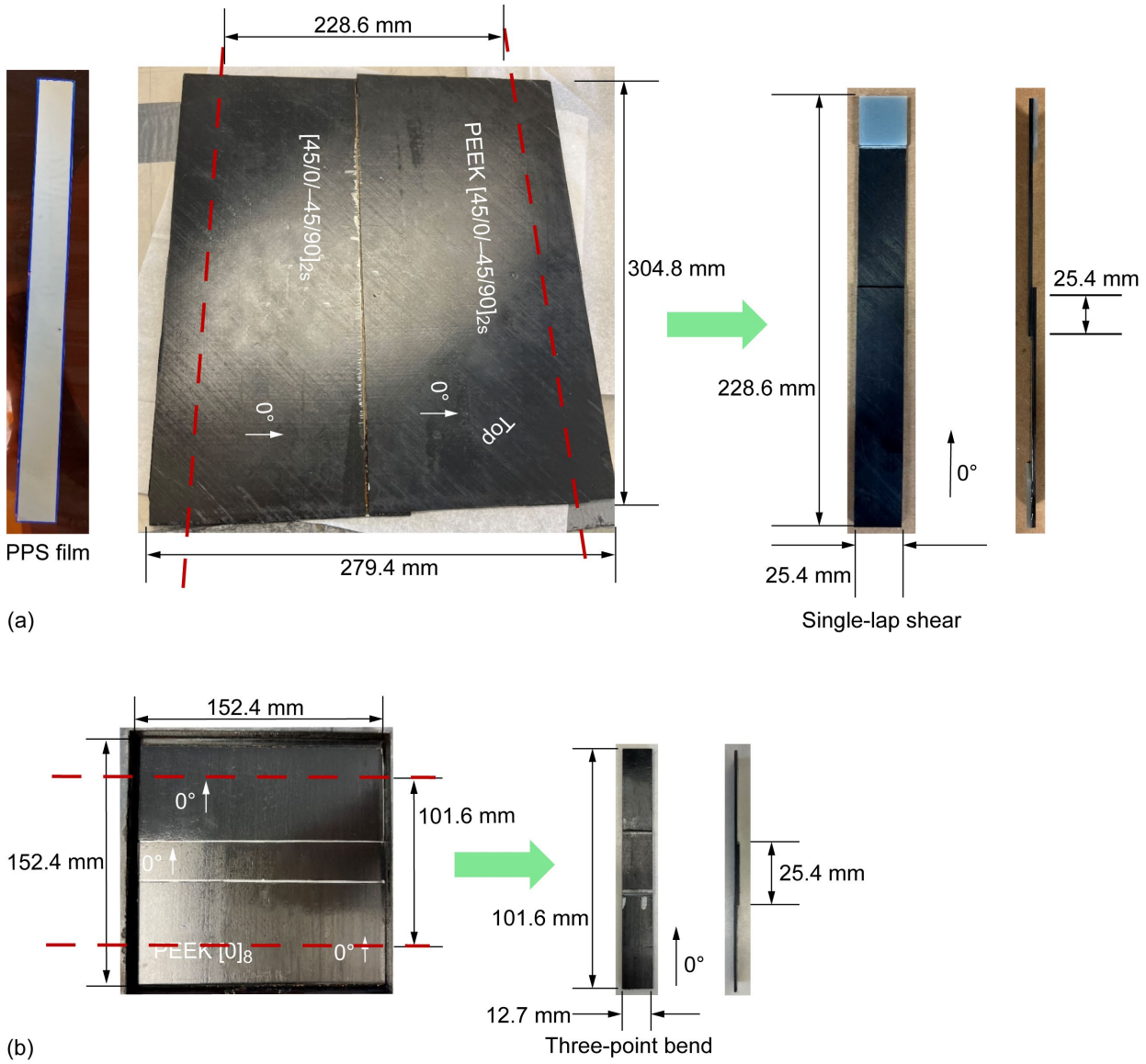

Figure 1.—Manufacturing and joining process for specimens of PEEK adherends with PPS interlayer composite joint specimens. (a) SLS joint. (b) Three-point bend joint.

Nominal dimensions for the SLS coupons were 25.3 mm wide by 229 mm long with a 25.4-mm overlap in the center joint. Nominal dimensions for three-point bend coupons were 12.7 mm wide by 102 mm long with a 25.4-mm doubler joined at the center. All adherends were AS4/PEEK, with the exception of a single hybrid joint design where the top and bottom plies of the AS4/PEEK $[45/0/–45/90]_{2s}$ panel were substituted with a ply of T700/LM-PAEK prepreg. This panel was used to investigate wh her having a similar material layer could help transition the entanglement and consolidation using LM-PAEK film in a gradient to the remaining PEEK adherend. The lap shear joint panel with LM-PAEK film interlayer was formed by pressing at 329 °C and 0.14 MPa for 1 h.

2.2 Modified Three-Point Bend Test

A modified three-point bend test developed at the NASA Langley Research Center was used to evaluate disassembly of the thermoplastic bond (Refs. 14 and 15). The modified test uses a skin and doubler configuration that are bonded together. A rod at the center of the setup applies force to the specimen to isolate the tipping moment and encourage debonding. A schematic of the general setup is shown in Figure 2.

The test was set up on an Instron® (Illinois Tool Works Inc.) 68FM–Retrofit testing system with the bend fixture positioned on a platform in the center. The force rod was machined from a 25-mm-nominal-diameter stainless steel rod to have a round edge of diameter 6.4 mm and was centered on the specimen. The support span rollers also had a diameter of 6.4 mm and a span of 64 mm. The thickness of the specimen was approximately 2.2 mm, maintaining an approximate 32:1 span-to-thickness ratio as required by ASTM Standard D7264 (Ref. 16). The displacement rate was set to 1.3 mm/min and force-displacement data were recorded by software on the Instron® system.

The full schematic of the Instron® three-point bend setup rig is shown in Figure 3.

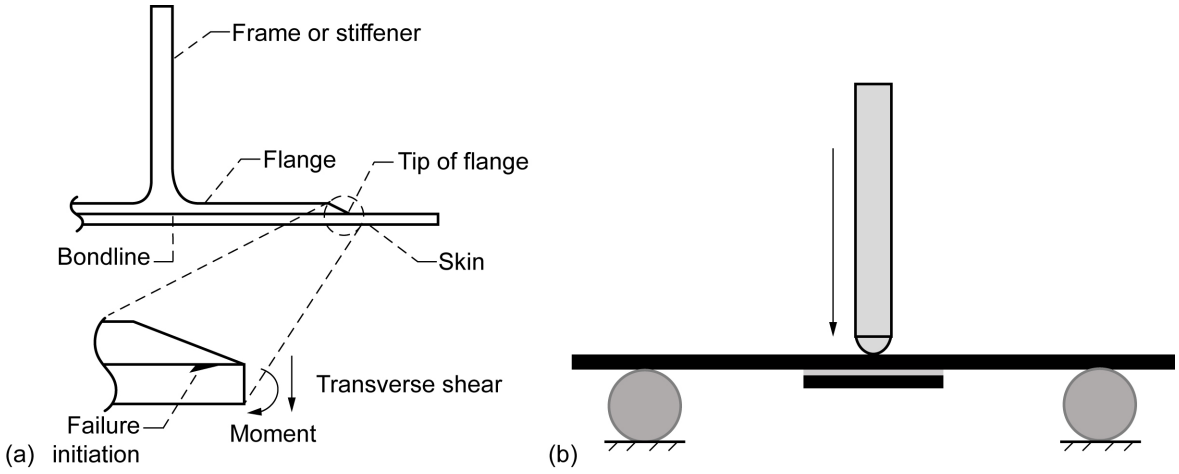

Figure 2.—Modified three-point bend test. (a) Anticipated failure mode at flange/skin interface (Ref. 14). (b) Test configuration serving as model.

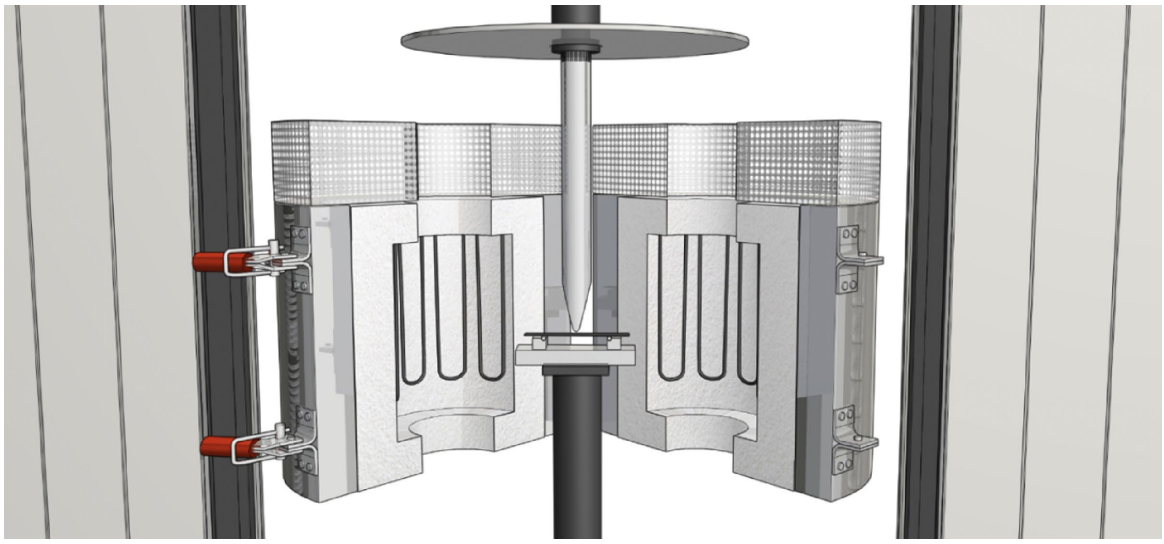

Figure 3.—Setup of modified three-point bend fixture and test on Instron® system.

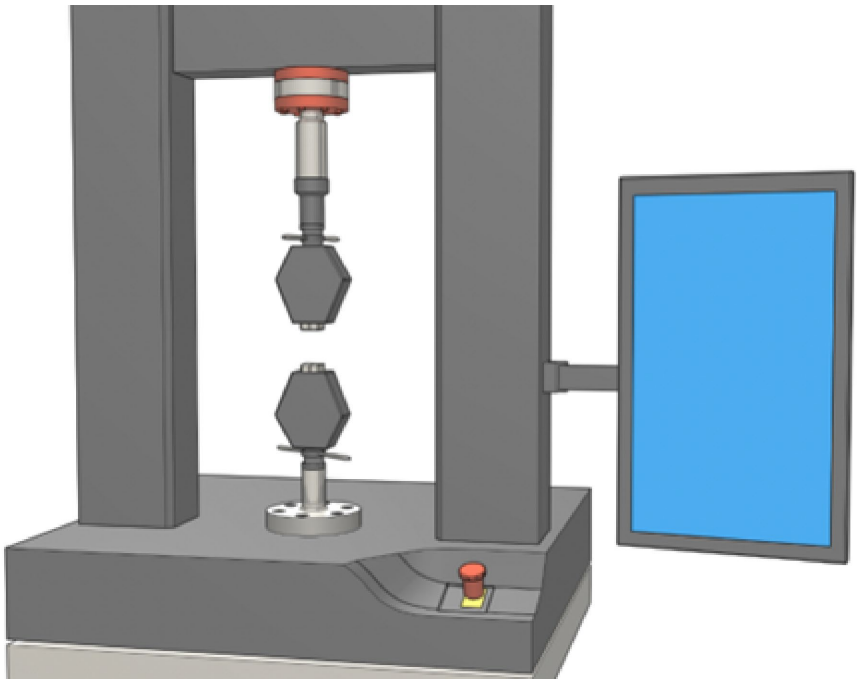

Figure 4.—SLS test setup on Instron® system (sample and furnace not shown).

2.3 Single-Lap Shear Test

To quantify the shear strength of thermoplastic joints, SLS tests were performed according to ASTM Standard D5868 (Ref. 17). Modifications to the standard test method included holding the displacement rate to 1.3 mm/min, rather than the suggested 13 mm/min, and increasing the PEEK adherend length from 102 to 127 mm long, making the final specimen 229 mm long. The length extension was required so the specimen would fit fully inside the furnace for ET tests. Each SLS specimen was tabbed on both ends for a more symmetric loading profile. The top grip fixture was an adjustable grip head, which allowed for realignment upon loading to ensure the specimen was being pulled in pure shear without twisting or contortion.

The full Instron® 68TM–50 diagram without the furnace configuration is pictured in Figure 4.

2.4 Thermal Screening

Thermal screening was necessary to ensure accurate temperature profiles of the specimen within the heating chamber. For both the SLS and three-point bend tests, the desired ET at the joint was 121 °C. ET three-point bend tests were carried out with an Applied Test Systems Series 3320 furnace (3,040 W, 45 A, maximum temperature 1,540 °C) and a practice specimen of PEEK $[0]_8$–PPS–PEEK $[0]_8$. High-temperature Type K thermocouples were wired and attached to the specimen in setup, as seen in Figure 5. Thermal testing revealed a ±3 °C offset between external and internal thermocouples.

Likewise, temperature screening was conducted for the SLS specimen test setup using an Applied Test Systems Series 3210 furnace (900 W, 7.8 A, max. temperature 900 °C). Practice specimens of PEEK $[45/0/–45/90]_{2s}$–PPS–PEEK $[45/0/–45/90]_{2s}$ were used for the SLS tests. High-temperature Type K thermocouples were wired to the specimen as shown in Figure 6. Steady-state temperature measurements revealed a ±4 °C offset between desired temperature at the center joint and the ambient readout, which could be accessed during ET testing.

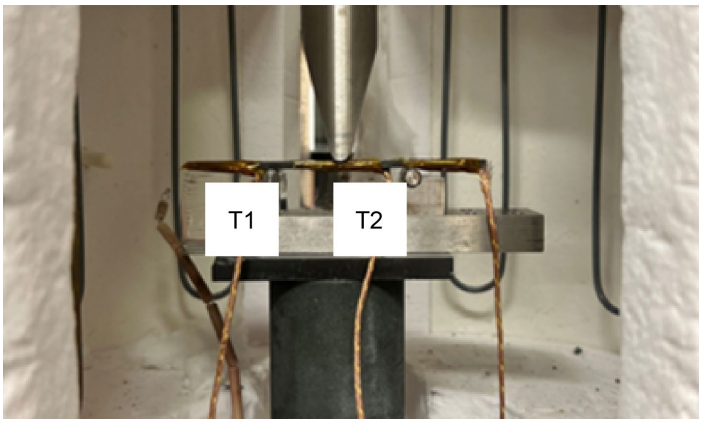

Figure 5.—Practice bend specimen for thermal testing showing placement of thermocouples T1 and T2. Furnace is open for photographing but closed during testing.

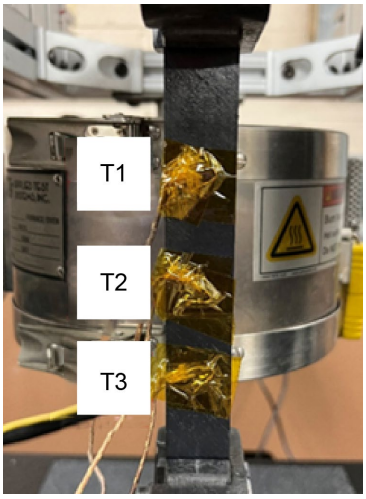

Figure 6.—Practice SLS specimen for thermal testing showing placement of thermocouples T1, T2, and T3. Furnace is open for photographing but closed during testing.

3.0 Results

3.1 Mechanical Testing

3.1.1 Three-Point Bend

Five bonded coupons were tested in a three-point bend configuration to determine disassembly force. A 27.5 percent higher force was required at ET than at RT, as noted in Table I and depicted in Figure 7. This was attributed to the PPS interlayer being above T_g (90 °C) in its rubbery state, which increases ductility at the bondline. At RT, the PPS is in its glassy state and as such behaves more brittle, resulting in a lower force required to break the bonded joint.

Because of similar trends with the SLS test, three-point bend testing was discontinued for the LM-PAEK interlayer material systems. This decision did not impact key trend investigations and saved manufacturing and testing time.

TABLE I.—AVERAGE MAXIMUM FORCE AND DISPLACEMENT AT FAILURE FOR THREE-POINT BEND SPECIMENS OF PEEK ADHERENDS WITH PPS FILM INTERLAYER

[ET is within ±3 °C; values are ±1 standard deviation.]

Property	Test temperature	
	RT, ~23 °C	ET, ~121 °C
Maximum force, N	55.5±9.0	70.8±9.3
Displacement at failure, mm	0.73±0.13	1.08±0.18

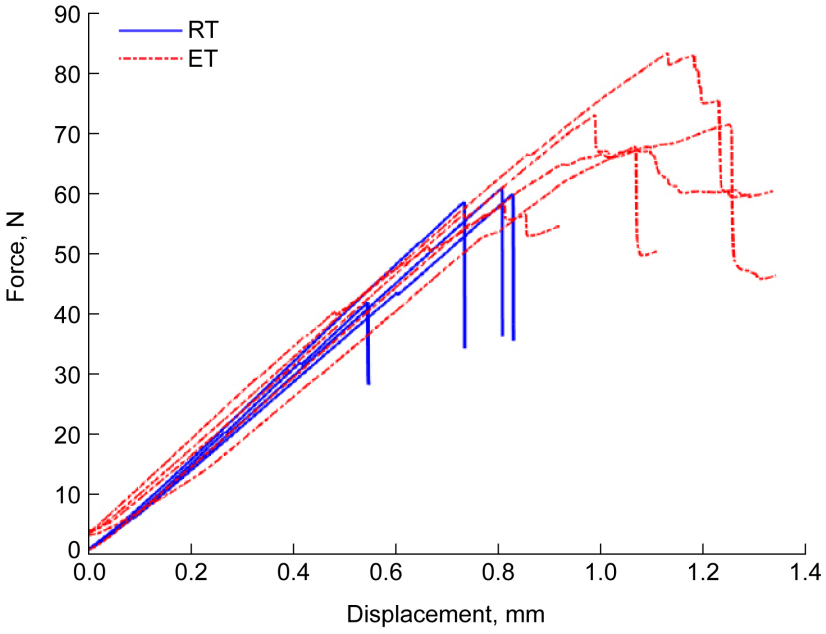

Figure 7.—Force versus displacement three-point bend specimens of PEEK adherends with PPS film interlayer at RT (23 °C) and ET (121 °C).

3.1.2 Single-Lap Shear

SLS specimens bonded with PPS film were loaded and tested at RT and ET, five specimens each. Results summarized in Table II and Figure 8 show that on average, there is a 66 percent higher maximum stress at failure at ET compared to RT. The ET samples also displaced 1.29 mm at failure compared to 0.86 mm at RT, highlighting that in the ET environment, PPS is in its rubbery state and behaves more ductile. At RT, the specimen is in its glassy regime and thus is more brittle and fails at a lower load.

TABLE II.—AVERAGE MAXIMUM STRESS AND DISPLACEMENT AT FAILURE FOR SLS SPECIMENS OF PEEK ADHERENDS WITH PPS FILM INTERLAYER

[ET is within ±3 °C; values are ±1 standard deviation.]

Property	Test temperature	
	RT, ~23 °C	ET, ~121 °C
Maximum stress, MPa	4.23±1.19	7.04±0.49
Displacement at failure, mm	0.86±0.18	1.29±0.14

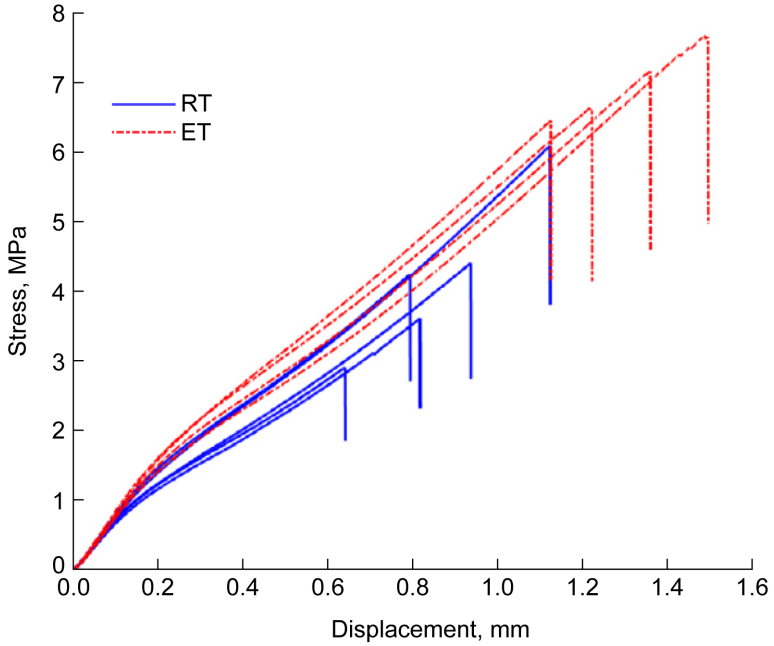

Figure 8.—Stress versus displacement for SLS specimens of PEEK adherends with PPS film interlayer at RT and ET.

For the PEEK adherend specimens bonded with LM-PAEK film, there was not a significant difference (average values within one standard deviation of each other) between maximum stress and displacement at failure in RT as compared to ET. The similarity of properties was expected, as the ET of 121 °C was below the T_g of the LM-PAEK (147 °C) film, meaning the material remained in the glassy state for both RT and ET tests. Tests above this T_g could not be completed because the T_g of PEEK is 143 °C, and therefore both the film and adherend would be rubbery, rendering SLS testing ineffective. Results are summarized in Table III and Figure 9.

TABLE III.—AVERAGE MAXIMUM STRESS AND DISPLACEMENT AT FAILURE FOR SLS SPECIMENS OF PEEK ADHERENDS WITH LM-PAEK FILM INTERLAYER

[ET is within ±3 °C; values are ±1 standard deviation.]

Property	Test temperature	
	RT, ~23 °C	ET, ~121 °C
Maximum stress, MPa	6.56±1.07	8.47±1.19
Displacement at failure, mm	1.09±0.21	1.4±0.18

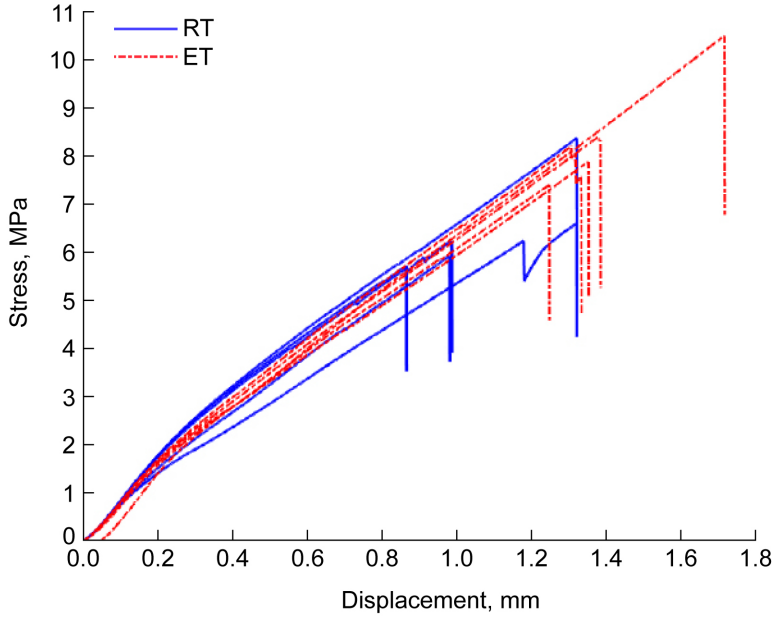

Figure 9.—Stress versus displacement for SLS specimens of PEEK adherends with LM-PAEK film interlayer at RT and ET.

Lastly, the hybrid PEEK/LM-PAEK adherends bonded with LM-PAEK film were tested in the SLS configuration, five specimens each for RT an ET. The outer plies of the adherend were LM-PAEK prepreg to increase the bonded strength of thermoplastic joint assembly. The results show that the specimens handled a much higher shear stress to failure, 34.6 MPa at RT, with similar behavior at ET. As noted previously, the ET of 121 °C was still below the T_g of both PEEK and LM-PAEK. There was a much higher displacement to failure as well, 5.38 mm at RT. Utilizing LM-PAEK as outer plies on the adherend reduced the film interface as a separate entity and increased entanglement between the two adherends. The weakest point of the composite matrix was no longer isolated to the film interface but was instead a few plies above or below. Results are recorded in Table IV and Figure 10. The failure mode is discussed in Section 3.2.2 of this report.

TABLE IV.—AVERAGE MAXIMUM STRESS AND DISPLACEMENT AT FAILURE FOR SLS SPECIMENS OF HYBRID PEEK/LM-PAEK ADHERENDS WITH LM-PAEK FILM INTERLAYER

[ET is within ±3 °C; values are ±1 standard deviation.]

Property	Test temperature	
	RT, ~23 °C	ET, (~121 °C)
Maximum stress, MPa	34.6±2.48	32.7±1.28
Displacement at failure, mm	5.38±0.39	5.14±0.2

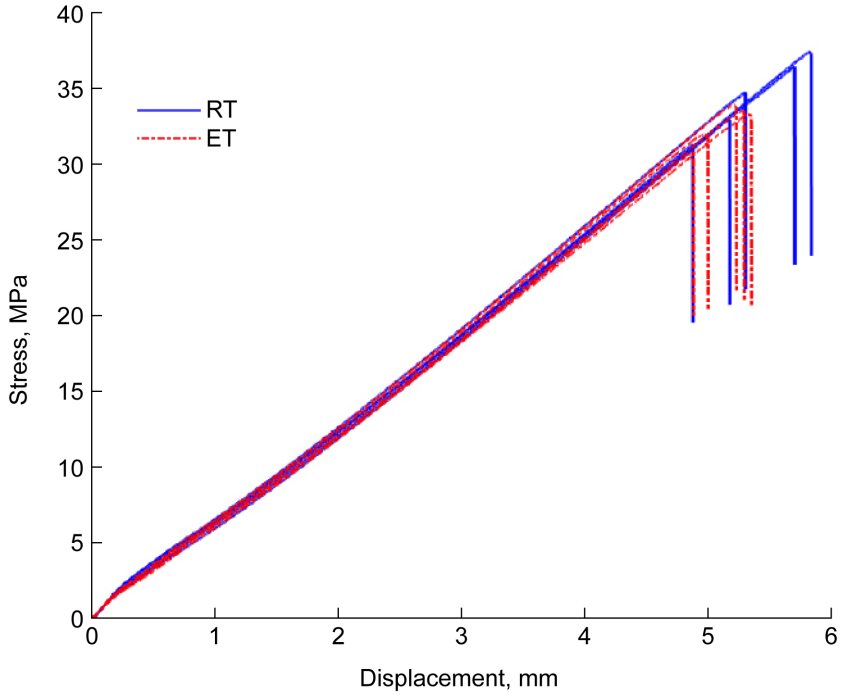

Figure 10.—Stress versus displacement plot for SLS specimens of hybrid PEEK/LM-PAEK adherends with LM-PAEK film interlayer at RT and ET.

The data demonstrate that joining PEEK with a dissimilar film, such as PPS or LM-PAEK, limits the maximum stress to a range of 3 to 8 MPa, with the LM-PAEK at the higher end of that range due to its similarity in chemical structure with PEEK. Co-consolidating LM-PAEK prepreg with the PEEK adherend drove the maximum stress to 34.6 MPa and displacement to 5.38 mm before failing at RT.

Fracture surfaces of the SLS coupons were evaluated to gain a better understanding of the advantages and disadvantages of each material.

3.2 Failure Modes

3.2.1 Three-Point Bend

The three-point bend specimen with a PPS film interlayer failed by peeling off from the edge of the doubler/skin interface, as desired. The tipping moment was large enough to peel the doubler off until it reached the center of the specimen. The PEEK adherend and doubler with a PPS film interlayer is shown prior to testing and after failure in Figure 11.

3.2.2 Single-Lap Shear

The SLS specimens were tested until failure. The adjustable grip head and a PPS interlayer sample prior to testing and after failure are shown in Figure 12.

As seen in Figure 12 and Figure 13, the PPS film failed adhesively at the film/adherend interface. This is desired for reassembly in that the adherend remained undamaged. However, the residual PPS film did not fully cover the bond area of the adherend. Greater coverage is required for reassembly, so an additional layer of film was deemed necessary prior to reassembly.

The same process was repeated for the LM-PAEK film with PEEK adherends. Similar adhesive failure trends were observed, as shown in Figure 14.

Lastly, the specimens with a hybrid PEEK/LM-PAEK adherend and LM-PAEK film were tested to failure. Fracture surfaces are shown in Figure 15. Note that ET was still below the T_g of LM-PAEK. Failure was more random and occurred within the adherend rather than at the joint interlayer surface.

This hybrid adherend provided opportunity for polymer chain entanglement between the LM-PAEK film and the adherend. As a result, the failure mode was much more catastrophic, unpredictable, and damaging to the adherend with the fracture surface composed of exposed carbon fiber rather than LM-PAEK film. Although this approach yielded a stronger bond, it is not amenable yet for reliable disassembly and reassembly of TPC applications because of the high amount of damage inflicted on the adherends.

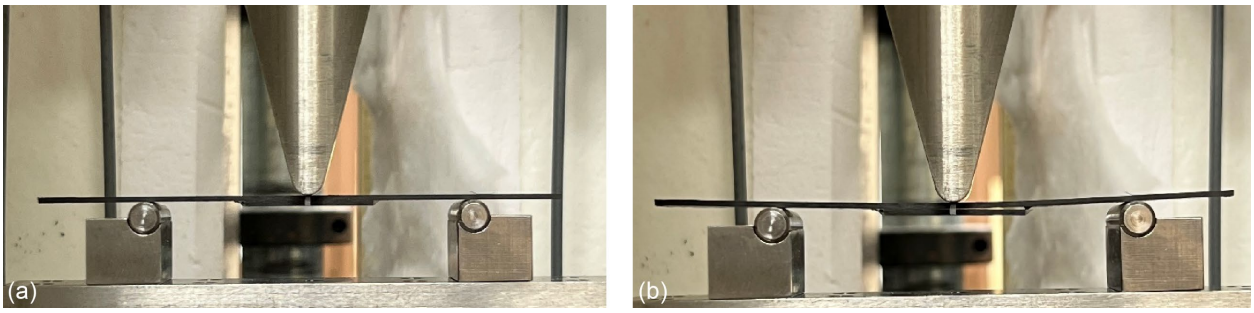

Figure 11.—Modified three-point bend test specimen of PEEK adherend and doubler with PPS film interlayer. (a) Prior to testing. (b) After failure.

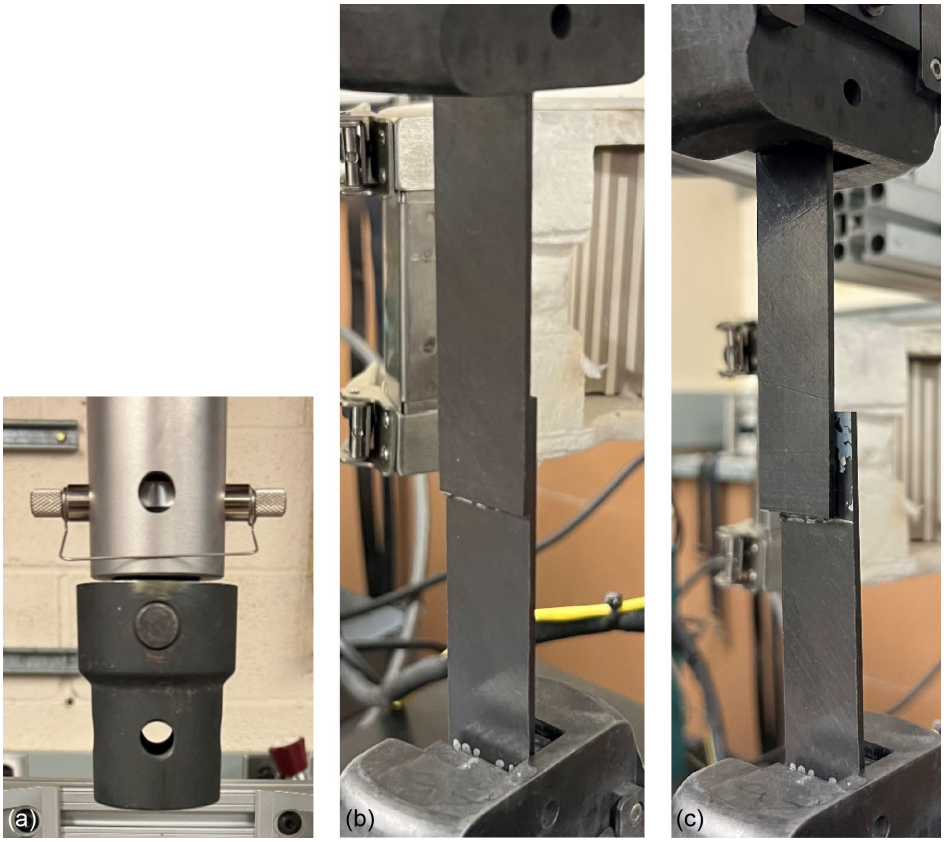

Figure 12.—SLS test setup. (a) Adjustable grip head. (b) Specimen of PEEK adherends with PPS film interlayer prior to testing. (c) Specimen after failure.

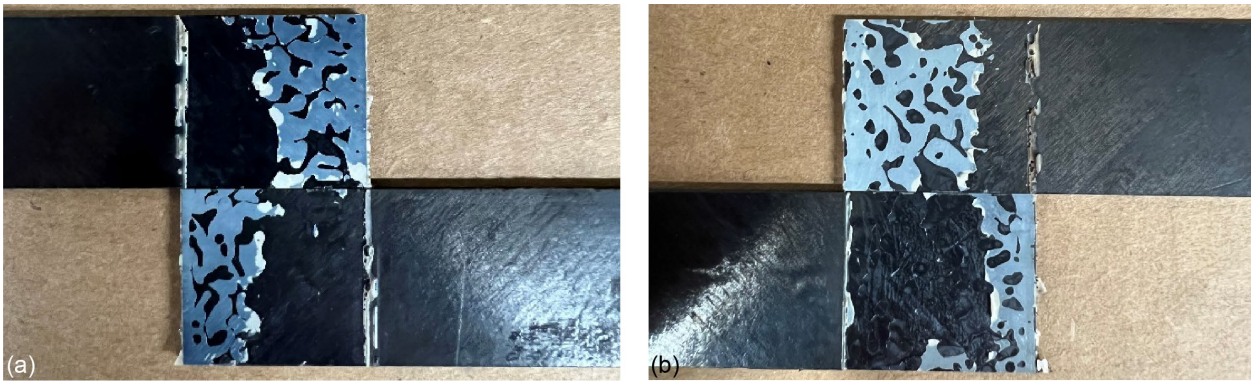

Figure 13.—Adhesive failure of broken SLS joints of PEEK adherends with PPS interlayer. (a) At RT. (b) At ET.

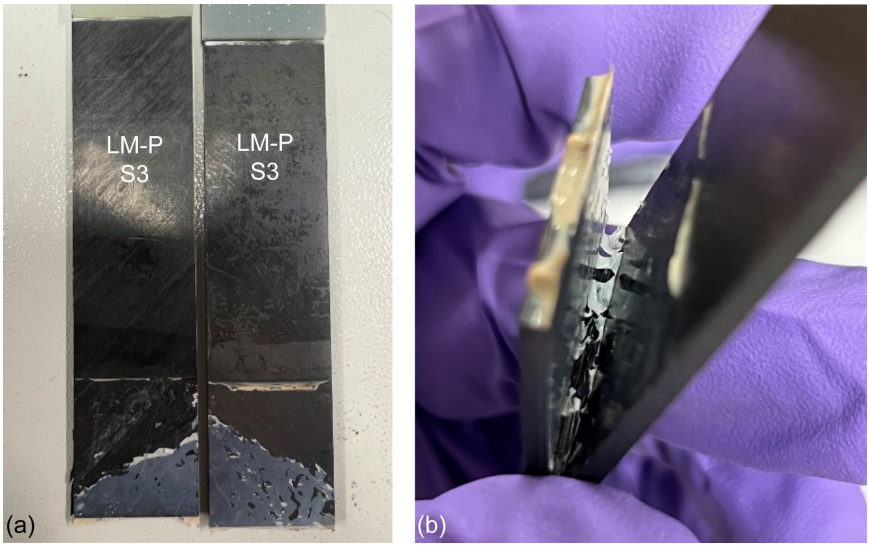

Figure 14.—Adhesive failure of broken SLS joints of PEEK adherends with LM-PAEK interlayer. (a) At RT. (b) At ET.

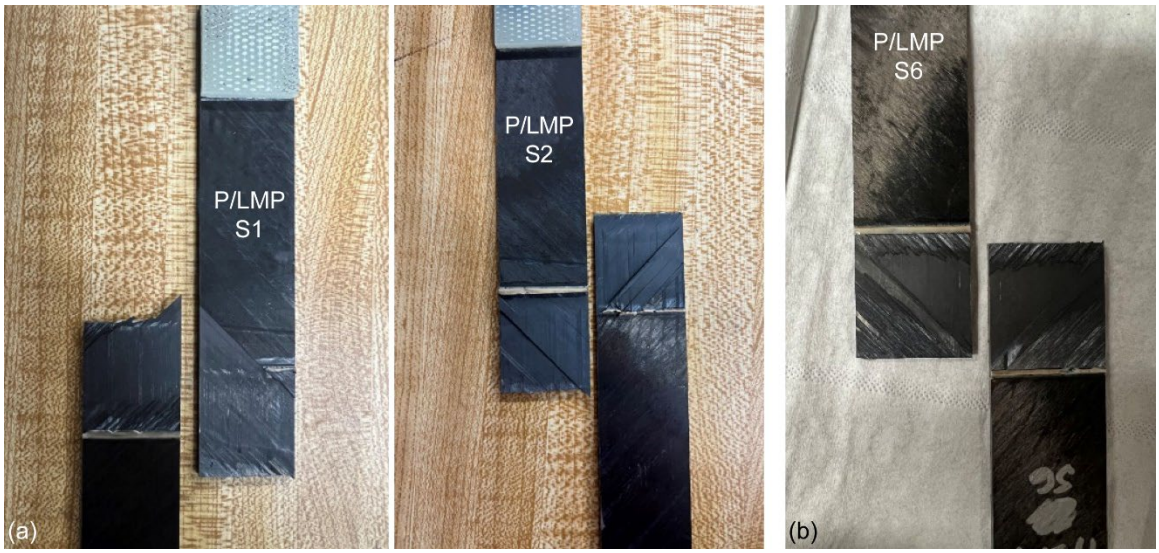

Figure 15.—Broken SLS joints using LM-PAEK interlayer with hybrid PEEK/LM-PAEK adherend. (a) At RT. (b) At ET.

4.0 Reassembly

After SLS testing, the coupons were preserved for reassembly purposes. A custom frame was built to hold the specimens in place and apply heat and pressure in the press. The coupons with PPS film interlayer were laid on top of each other without making any changes to the joint surface, and no additional material was added. Steel bars were overlaid to allow for even pressure distribution and heat conduction. The coupons were pressed at the same conditions as initial joining. A flowchart of this reassembly process is documented in Figure 16.

The glass fiber tabs and glue melted as expected but the joint was reformed. Once rejoined, two coupons were tested again in the SLS configuration, and results are summarized in Figure 17.

The reassembled coupons had a similar mechanical strength at RT compared to the original coupons. A greater displacement to failure and lower modulus indicates higher compliance, possibly due to damage

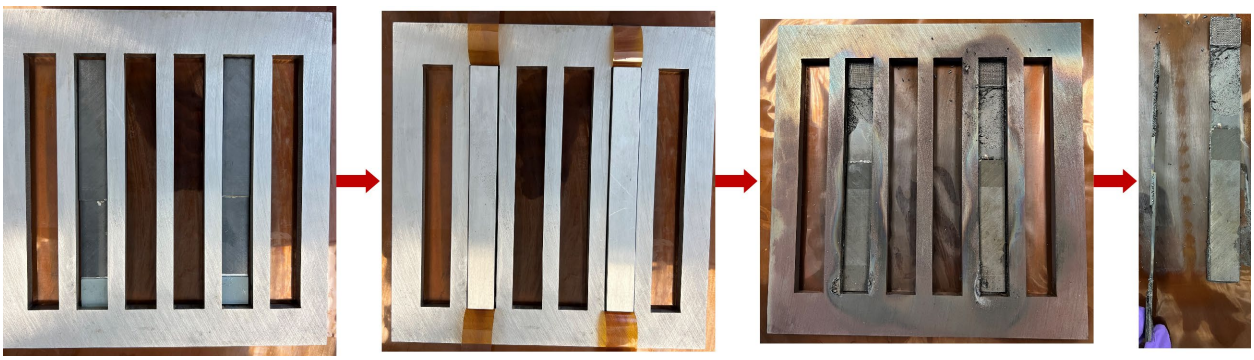

Figure 16.—Reassembly of SLS coupons of PEEK adherends with PPS film interlayer.

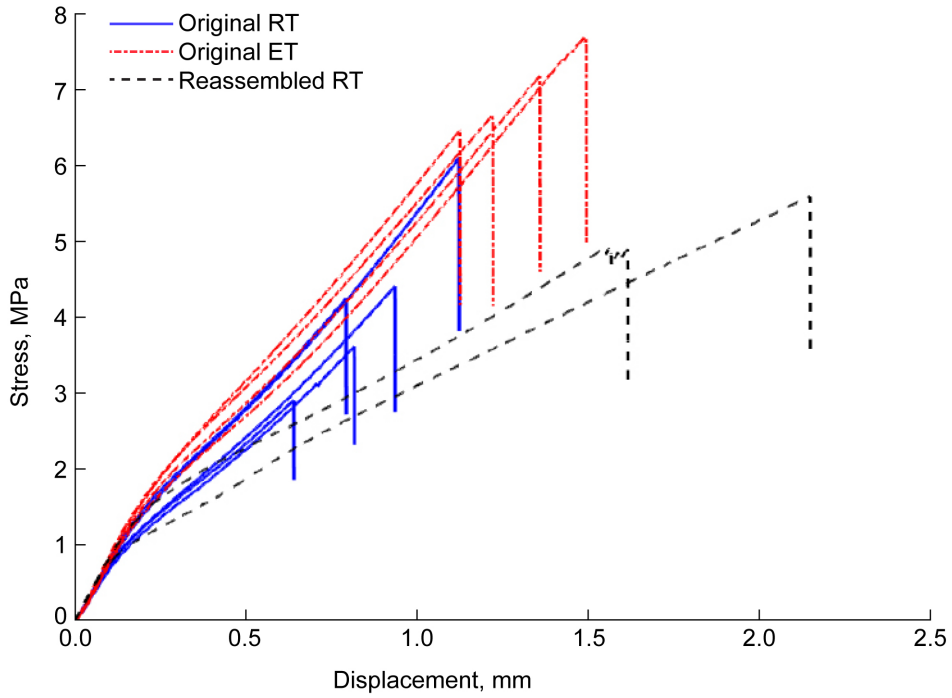

Figure 17.—Stress versus displacement for reassembled SLS specimens of PEEK adherends with PPS film interlayer at RT compared to those of original SLS specimens at RT and ET.

Figure 18.—Thermal degradation and flowout of PPS film in broken sample.

of the adherends and tabs incurred during reassembly or variation in charred gripping tabs. Upon separation, the surfaces appeared to be smooth and lacked residual PPS film, as shown in Figure 18. From literature, it is known that PPS has poor thermal stability under heat treatment, which leads to degradation through chain scission, extension, branching, and crosslinking, reducing processability and performance (Ref. 18). In this case, thermal degradation and flowout would prevent further reassembly, so a new film was required before subsequent joining.

A similar process was repeated for the reassembly of coupons with an LM-PAEK film interlayer. However, this time an additional layer of fresh LM-PAEK film with the same thickness was added in the 25- by 25-mm overlap to improve joint fidelity. This approach was taken for both the PEEK and hybrid PEEK/LM-PAEK adherends and is outlined in Figure 19.

SLS results of the specimens of PEEK adherends with LM-PAEK film are shown in Figure 20, and the data for specimens of hybrid PEEK/LM-PAEK adherend with LM-PAEK film are shown Figure 21.

There was not a significant difference in maximum stress values for the rejoined PEEK adherends with LM-PAEK film as compared to the original maximum stress values at RT. This was because the joint adhesively failed and carried the load, so it behaved similarly. However, a different trend was observed with the specimen having the hybrid PEEK/LM-PAEK adherend.

The reassembled hybrid PEEK/LM-PAEK coupons were significantly weaker than the pristine coupons. This was due to the damage inflicted during disassembly, as previously detailed. The broken specimens are shown in Figure 22.

As with the disassembly of the as-manufactured test coupons, the fracture surfaces of the reassembled coupons indicate adhesive failure of the LM-PAEK film bonded to PEEK adherends, whereas fiber breakage was observed with the hybrid PEEK/LM-PAEK adherends. Flowout of the film from the bondline was an issue, as very little residual LM-PAEK film remained at the interface, highlighting the need for optimization of press parameters to create a thermoplastic joint with high fidelity. It is important to note that in each case the reassembled coupons had a lower slope than the original. This was most likely due to slippage in the grips during testing because the tabs were charred and damaged during the reassembly process, rather than a structural change of the polymer interlayer itself.

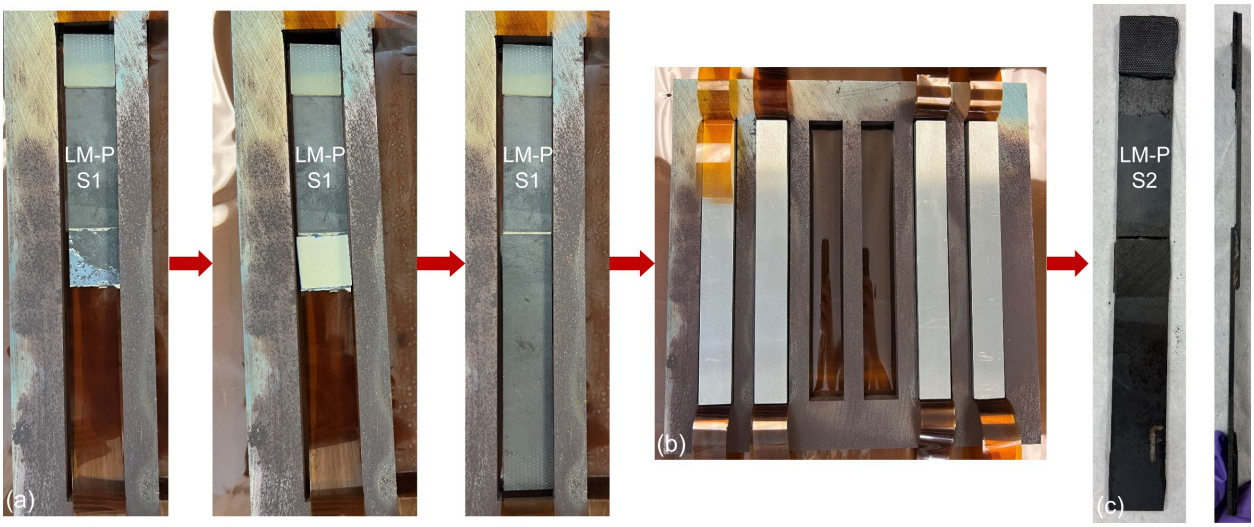

Figure 19.—Reassembly of SLS specimens. (a) Addition of new LM-PAEK film interlayer. (b) Addition of platens for pressing. (c) Reformed joint after pressing.

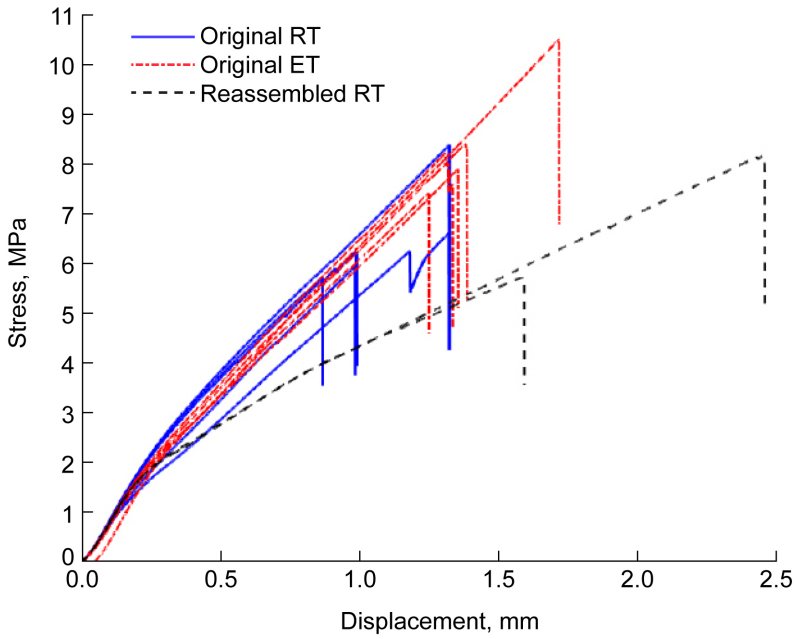

Figure 20.—Stress versus displacement for reassembled PEEK adherends with LM-PAEK film interlayer SLS specimens at RT compared to original SLS specimens at RT and ET.

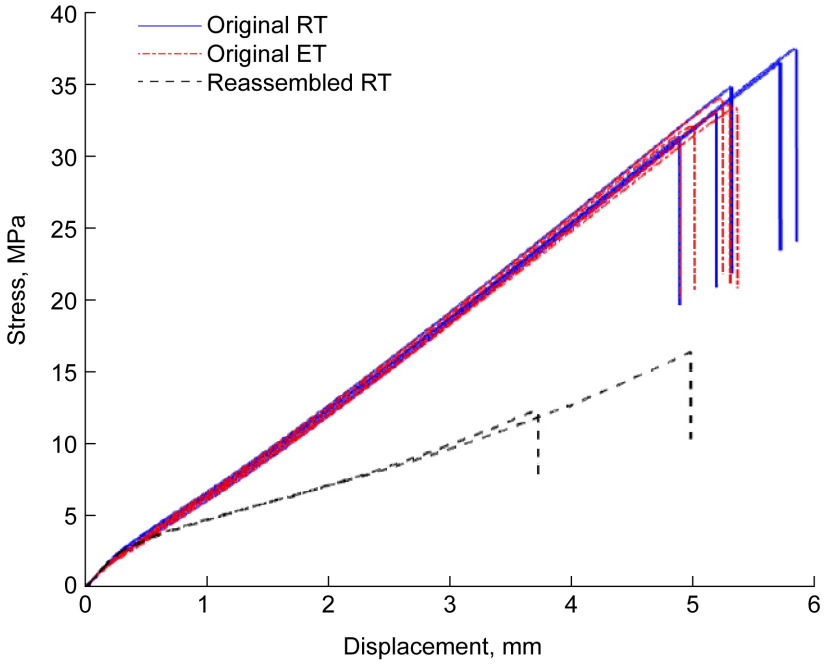

Figure 21.—Stress versus displacement for reassembled hybrid PEEK/LM-PAEK adherends with LM-PAEK film interlayer SLS specimens at RT compared to original SLS specimens at RT and ET.

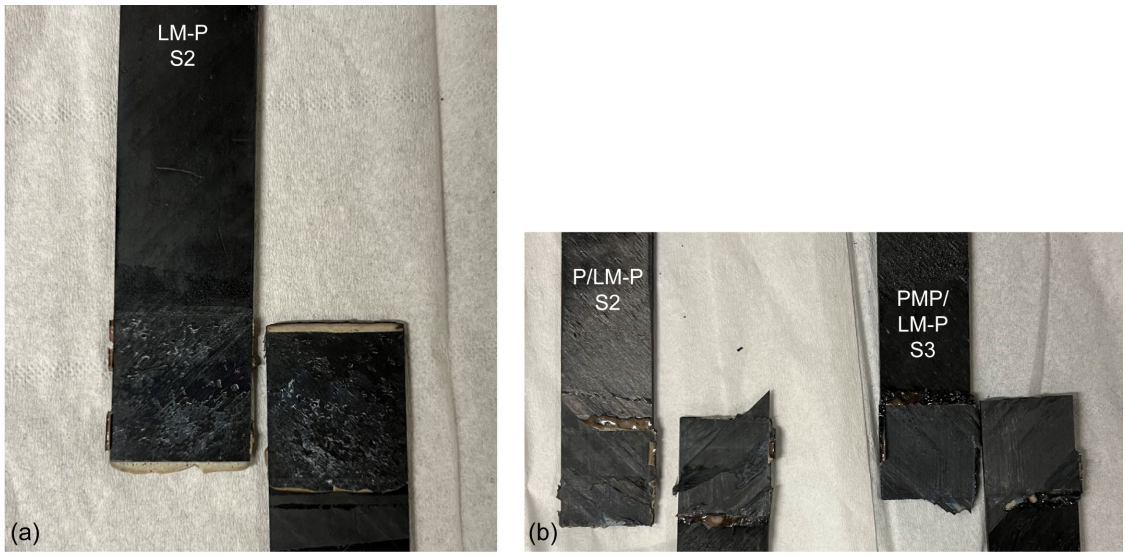

Figure 22.—Broken SLS joints using LM-PAEK interlayer at RT. (a) PEEK adherends with LM-PAEK interlayer. (b) Hybrid PEEK/LM-PAEK adherends.

5.0 Conclusions

This work demonstrated the feasibility of joining, disassembly, and reassembly of thermoplastic composite bonds in a hot press using both polyphenylene sulfide (PPS) and low-melt polyaryl ether ketone (LM-PAEK) film interlayers. Necessary balancing shims, a reassembly frame, adjustable grip heads, and furnaces were set up and developed to complete this work. Single-lap shear and three-point bend coupons for each material were tested at room temperature (RT) (23 °C) and elevated temperature (ET) (121 °C) to understand how mechanical behavior changes with temperatures below and above the glass transition temperature of PPS. When the failure was isolated to the film, specimens at ET required a higher force and stress to failure compared with those at RT because of the increased ductility and toughness of the PPS film in its rubbery state, as opposed to brittle behavior in its glassy state.

Although reassembly of the bonded joint was demonstrated, additional film interlayers will likely be required with each subsequent reassembly to maintain joint fidelity. Future work will focus on reducing the loss of film at the interlayer and investigating alternative joining methods.

References

1. Alshammari, Basheer A., et al.: Comprehensive Review of the Properties and Modifications of Carbon Fiber-Reinforced Thermoplastic Composites. Polymers, vol. 13, no. 15, 2021, p. 2474.
2. Vodicka, Roger: Thermoplastics for Airframe Applications: A Review of the Properties and Repair Methods for Thermoplastic Composites. DSTO–TR–0424, 1996.
3. Zeyrek, B.Y., et al.: Review of Thermoplastic Composites in Aerospace Industry. Int. J. Eng. Tech. Inf., vol. 3, 2022, pp. 1–6.
4. August, Zachary, et al.: Recent Developments in Automated Fiber Placement of Thermoplastic Composites. SAMPE J., vol. 50, no. 2, 2014, pp. 30–37.
5. Barroeta Robles, J., et al.: Repair of Thermoplastic Composites: An Overview. Adv. Manuf.: Polym. Compos. Sci., vol. 8, no. 2, 2022, pp. 68–96.
6. de Weert, Loic: Disassembly of Fusion Bonded Thermoplastic Composite Joints Aided by Induction Heating: Effects of Induction Heating on Disassembly Force and Damage Patterns. Master's Thesis, Delft Univ. of Technology, 2021.
7. Frederick, Harry; Li, Wencai; and Palardy, Genevieve: Disassembly Study of Ultrasonically Welded Thermoplastic Composite Joints via Resistance Heating. Materials, vol. 14, no. 10, 2021, p. 2521.
8. Palardy, Genevieve, et al.: A Study on Amplitude Transmission in Ultrasonic Welding of Thermoplastic Composites. Compos. Part A Appl. Sci. Manuf., vol. 113, 2018, pp. 339–349.
9. Palardy, Genevieve; and Villegas, Irene Fernandez: On the Effect of Flat Energy Directors Thickness on Heat Generation During Ultrasonic Welding of Thermoplastic Composites. Compos. Interfaces, vol. 24, no. 2, 2017, pp. 203–214.
10. Kirby, Madeline; Naderi, Armaghan; and Palardy, Genevieve: Predictive Thermal Modeling and Characterization of Ultrasonic Consolidation Process for Thermoplastic Composites. J. Manuf. Sci. Eng., vol. 145, no. 3, 2023, p. 031009.
11. Li, Wencai; Frederick, Harry; and Palardy, Genevieve: Multifunctional Films for Thermoplastic Composite Joints: Ultrasonic Welding and Damage Detection Under Tension Loading. Compos. Part A Appl. Sci. Manuf., vol. 141, 2021, p. 106221.
12. Haq, Mahmoodul, et al.: Tailorable Adhesives for Multi-Material Joining, Facile Repair and Re-Assembly. Proceedings of the American Society for Composites 2015—Thirtieth Technical Conference, Michigan State University, East Lansing, MI, 2019.

13. Koutras, N.; Villegas, I.F.; and Benedictus, R.: Influence of Temperature on Strength and Failure Mechanisms of Resistance Welded Thermoplastic Composites Joints. 20th International Conference on Composite Materials, Copenhagen, Denmark, 2015.
14. Minguet, P.J.; and O'Brien, T.K.: Analysis of Test Methods for Characterizing Skin/Stringer Debonding Failures in Reinforced Composite Panels. Composite Materials: Testing and Design: Twelfth Volume, ASTM STP1274, R.B. Deo and C.R. Saff, eds., American Society for Testing and Materials, West Conshohocken, PA, 1996, pp. 105–124.
15. Selvarathinam, Alex S., et al.: Validation of Floating Node Method Using Three-Point Bend Doubler Under Quasi-Static Loading. AIAA 2019–1549, 2019.
16. ASTM D7264: Standard Test Method for Flexural Properties of Polymer Matrix Composite Materials. ASTM International, West Conshohocken, PA, 2021.
17. ASTM D5868: Standard Test Method for Lap Shear Adhesion for Fiber Reinforced Plastic (FRP) Bonding. ASTM International, West Conshohocken, PA, 2014.
18. Yan, Peng, et al.: Investigation on Thermal Degradation Mechanism of Poly (Phenylene Sulfide). Polym. Degrad. Stab., vol. 197, no. 109863, 2022.